Liquid Flow on a Rotating Disk Prior to Centrifugal Atomization and Spray Deposition

Y.Y. ZHAO, M.H. JACOBS, and A.L. DOWSON

Video observations of the flow patterns that develop on a rotating disk during centrifugal atomization and spray deposition, and subsequent metallographic studies conducted on solid skulls removed from the disk after processing, have indicated a circular discontinuity or hydraulic jump, which is manifested by a rapid increase in the thickness of the liquid metal and by a corresponding decrease in the radial velocity. A mathematical model has been developed that is capable of predicting both the occurrence and location of the jump, and the associated changes in the thickness profile and in the radial and tangential velocities of the liquid metal. Good correlations have been observed between model predictions and the flow patterns observed on the skull after atomization, and the effects of changes in material and operational parameters such as kinematic viscosity, volume flow rate, metallostatic head, and disk rotation speed have been quantified. Liquid metal flow is controlled primarily by the volume flow rate and by the metallostatic head prior to the hydraulic jump and by the centrifugal forces after the jump. The implications of these observations in terms of the atomization process are discussed.

I. INTRODUCTION

THE potential benefits of spray forming processes in producing microstructurally refined, chemically homogeneous, near-net-shaped components are well documented.[1,2] In this respect, spray forming processes are known to offer both commercial and technological advantages over traditional cast-wrought processing routes, particularly in the processing of some of the more advanced materials of current interest to the aerospace industry. Consistent with these advantages, and driven by the need to reduce manufacturing costs, aero-engine manufacturers are currently exploring the possibility of using spray forming technology as a means of producing low cost preforms as a precursor to the manufacture of ring and casing components.[3,4,5] The majority of spray forming processes developed to date, however, use high pressure gas, either Ar or N_2, to atomize the liquid metal stream, and as such the materials produced can be prone to problems from gas entrapment and postspray thermal-induced porosity.[6,7] As a consequence, there has been a growing interest in alternative spray forming technologies that can be operated in the absence of a gaseous environment. Based on a concept originally proposed by Singer and Kisakurek[8] and subsequently developed commercially by Osborne Metals (subsequently Aurora Steels),[9] the centrifugal atomization and spray deposition process uses a rapidly rotating copper disk or cup to both break up the metal stream and direct the flow of molten metal droplets onto the inner surface of a former or collector.[10–15] As such, the process negates the need for a high pressure gas stream and the system can be configured to operate either under reduced pressures or in a vacuum environment. In this respect, the process offers both economic and technical advantages over gas assisted deposition processes in that the problems associated with gas entrapment are virtually eliminated and processing costs are reduced because there is no longer the need to use large quantities of expensive process gases. In addition, further technological advantages stem from the greater flexibility in controlling droplet size distribution, and hence microstructural development, and from the ability to produce preforms with both internal and external shape.

The microstructures developed during centrifugal atomization and deposition are governed primarily by the mass flow rate, and by the temperature, velocity, and size distribution of the atomized droplets impinging on the substrate. As such, they are largely determined by the behavior of the liquid metal as it interacts with the atomizing disk, and by the fluid flow conditions that develop as a result of disk rotation. Although centrifugal atomization of water-based liquids and slurries has been extensively studied, primarily within the food, chemical, and agricultural industries,[16,17] the more stringent requirements regarding mass flow rate, disk rotation speed, and droplet size distribution mean that these studies are not directly transferable to the atomization of liquid metals. The situation is further exacerbated by the extreme temperatures involved and by the need to control the amount of solidification prior to deposition. As a consequence, disk rotation speeds tend to be much higher, typically in excess of 5000 rpm, with the mass flow rate being controlled to yield droplet size distributions less than approximately 200 μm. This ultimately results in higher tangential and radial velocities, and a corresponding reduction in the thickness or height of liquid metal on the disk, primarily due to the higher centrifugal force. Such increases in radial velocity are, however, not infinitely sustainable. Preliminary video observations of liquid Ti-48Al-2Mn-2Nb flow on the disk during centrifugal atomization, as shown in Figure 1, have indicated a radial or circular discontinuity in the flow pattern that is manifested by an abrupt increase

Y.Y. ZHAO, formerly Research Fellow, IRC in Materials for High Performance Applications, The University of Birmingham, Edgbaston, Birmingham B15 2TT, United Kingdom, is Lecturer, Materials Science and Engineering, Department of Engineering, The University of Liverpool, Liverpool L69 3BX, United Kingdom. M.H. JACOBS, Deputy Director, and A.L. DOWSON, Researcher Fellow, are with IRC in Materials for High Performance Applications, the University of Birmingham.

Manuscript submitted October 28, 1997.

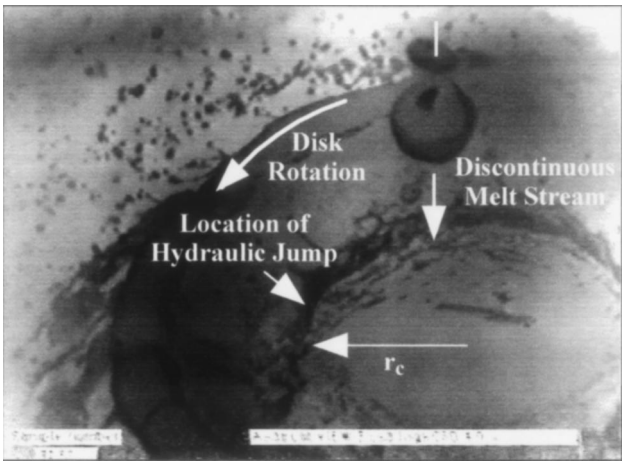

Fig. 1—Video image showing hydraulic jump in the flow of liquid metal on the disk during the centrifugal atomization of Ti-48Al-2Mn-2Nb.

in the thickness of the liquid metal on the disk and is accompanied by a corresponding reduction in the radial velocity. This phenomenon is referred to as a hydraulic jump in fluid mechanics,[18,19] and clearly has important implications regarding the atomization process and the subsequent control of droplet size distribution and microstructural morphology.

Although the hydraulic jump phenomenon that results from a liquid jet impinging normally on a stationary planar surface has been studied for more than 3 decades,[20–24] the phenomenon has not been reported in the case of liquid jets interacting with nonstationary or rotating substrates. Current understanding of the hydraulic jump is limited, and exact theoretical and mechanistic descriptions of the energy changes and the transient flow conditions within the vicinity of the jump are not available. Fortunately, since the region affected by the jump tends to be very narrow, these effects can be largely neglected in the analysis, with flow at either side of the jump being considered in terms of the conservation of energy, mass, and momentum. The exact solution of the conservation equations, particularly in the case of problems involving free surfaces and discontinuous flow, however, invariably requires the application of complex numerical procedures and access to powerful computational fluid dynamics software and computing facilities. As a consequence, approximate analytical solutions have been sought and have been used to provide a better insight into the mechanisms by which the operating conditions influence liquid behavior. The steady laminar flow of a viscous, incompressible fluid in a region close to a rapidly rotating disk is a classic problem in fluid mechanics, which has been considered by a number of workers.[25–28] Neglecting heat transfer between the liquid and the disk, the problem can generally be considered in terms of a set of ordinary differential equations derived from the Navier–Stokes and the conservation of mass equations. On this basis, approximate solutions can be obtained by substituting trial functions for each of the velocity components, which satisfy the boundary conditions and minimize the residuals of the equations.[28] Von Kármán[25] first examined this problem and gave an approximate solution based on an integral approach in which the velocity components were approximated by low-degree polynomials. This analysis was subsequently modified by Cochran[26] to include exponential functions and a more exact numerical solution in which the velocity components were expressed in terms of a series of powers of these functions. These solutions were further improved by Stuart,[27] and more recently, a simplified solution based on the use of trial functions has been presented by Ariel[28] without any trade-off in accuracy. All of the solutions presented to date, however, have been concerned with a rotating disk fully immersed in an originally stationary liquid. As such liquid velocity is controlled solely by the centrifugal forces generated by the rotating disk. In centrifugal atomization, since the liquid metal is poured continuously on to the surface of the disk, flow is also dependent on the pouring distances, which determines the initial axial velocity of the liquid stream at the point of impact. Equations describing the height, radial, and tangential velocities of liquid metal on the disk during atomization have been derived by Zhao *et al.*[29] assuming a balance between centrifugal and viscous forces caused by the nonuniformly distributed velocities. These equations, however, are only applicable when tangential slippage is small, *i.e.*, when the tangential velocity of the liquid metal is similar to that of the disk. Since slippage tends to increase with decreasing disk radius and rotation speed, and with increasing liquid volume flow rate, the applicability of these equations is limited. The model also fails to take into account the effects of different pouring distances and the occurrence of a hydraulic jump. The current article describes a mathematical model that is capable of predicting both the occurrence and location of the hydraulic jump, and the associated changes in the height profile, and in the radial and tangential velocities of the liquid metal on the disk. The implications of the model in terms of the atomization process are discussed, and quantitative information is presented relating to the effects of changes in the atomization conditions on the height, axial, and tangential velocities of the liquid metal on an atomizing disk.

II. MODEL DERIVATION

A. *Statement of Problem*

In centrifugal atomization, a controlled jet of liquid metal is directed under gravity on to the center of a rapidly rotating disk where it is accelerated both radially and tangentially toward the edge of the disk prior to atomization. As a result, the liquid metal will adopt a height profile that will ultimately be determined by the kinematic viscosity of the liquid metal and by the gravitational, frictional, and centrifugal forces acting between the liquid metal and the disk. Assuming that flow is axisymmetric and that it is accompanied by a hydraulic jump at a critical radius r_c, the liquid profile may be represented schematically by Figure 2. As indicated, the height of liquid metal on the disk before and after the hydraulic jump, denoted δ_1 and δ_2, respectively, varies with radius. Similarly, the radial, tangential, and axial components of the liquid velocity, denoted u, v, and w, respectively, vary with both radius r and axial distance z from the disk surface.

In developing the mathematical model, the following assumptions have been made.

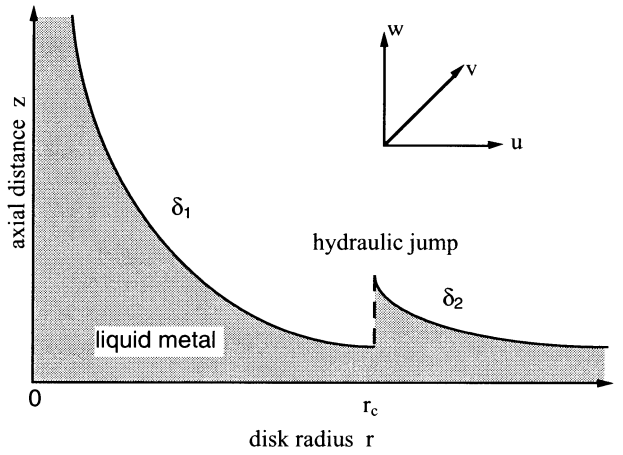

Fig. 2—Schematic height profile of the liquid metal on an atomizing disk, assuming a hydraulic jump takes place at a radius of r_c.

(1) Liquid metal flow to the center of the disk is uniform and continuous and maintains a constant volume flow rate throughout the atomization process.
(2) The velocity distribution and height of liquid metal on the disk are axisymmetric and do not vary in the tangential direction.
(3) The liquid metal maintains a constant temperature above its melting point during atomization without thermal loss.
(4) The liquid metal acts as a Newtonian fluid with a constant viscosity.
(5) Due to frictional effects, slippage at the interface between the liquid metal and the disk is zero, and the liquid metal at the interface moves at the same tangential velocity as the disk.
(6) The surface tension of the liquid metal is negligible, such that the problem resolves to that of a rotating disk immersed in a large volume of liquid metal.

Based on the preceding considerations, and neglecting the effects of heat transfer between the liquid metal and the disk, liquid metal flow is determined by the Navier–Stokes equations of momentum conservation and by the equation of mass conservation, which in cylindrical coordinates can be written as[19]

$$\left.\begin{aligned}
&u\frac{\partial u}{\partial r}+\frac{v}{r}\frac{\partial u}{\partial \theta}+w\frac{\partial u}{\partial z}-\frac{v^2}{r}=-\frac{1}{\rho}\frac{\partial p}{\partial r}\\
&\quad+\nu\left(\nabla^2 u-\frac{u}{r^2}-\frac{2}{r^2}\frac{\partial v}{\partial \theta}\right)\\
&u\frac{\partial v}{\partial r}+\frac{v}{r}\frac{\partial v}{\partial \theta}+w\frac{\partial v}{\partial z}+\frac{uv}{r}=-\frac{1}{\rho r}\frac{\partial p}{\partial \theta}\\
&\quad+\nu\left(\nabla^2 v-\frac{v}{r^2}-\frac{2}{r^2}\frac{\partial u}{\partial \theta}\right)\\
&u\frac{\partial w}{\partial r}+\frac{v}{r}\frac{\partial w}{\partial \theta}+w\frac{\partial w}{\partial z}=-\frac{1}{\rho}\frac{\partial p}{\partial z}+\nu\nabla^2 w\\
&\frac{1}{r}\frac{\partial}{\partial r}(ru)+\frac{1}{r}\frac{\partial v}{\partial \theta}+\frac{\partial w}{\partial z}=0
\end{aligned}\right\}\quad[1]$$

where r is the radial distance from the axis of rotation of the disk, θ is the polar angle in the direction of rotation, z is the axial distance from the disk, p is the pressure, ρ is the density, ν is the kinematic viscosity of the liquid, and ∇^2 is a mathematical operator defined as

$$\nabla^2 \equiv \frac{\partial^2}{\partial r^2}+\frac{1}{r}\frac{\partial}{\partial r}+\frac{1}{r^2}\frac{\partial^2}{\partial \theta^2}+\frac{\partial^2}{\partial z^2}$$

At the interface between the liquid and the rotating disk, the radial and axial velocities of the liquid tend to zero, whereas the tangential velocity is determined by the speed of disk rotation. The radial and tangential components vanish on moving vertically away from the disk, whereas the axial component must tend toward a finite value in order to preserve continuity and to balance the radial flow of liquid. On this basis, the initial boundary conditions can be specified such that

$$u=0,\ v=\omega r,\ w=0 \qquad \text{at } z=0$$

$$u=0,\ v=0,\ w\neq 0,\ \frac{\partial u}{\partial z}=0,\ \frac{\partial v}{\partial z}=0,\ \frac{\partial w}{\partial z}=0 \qquad \text{at } z=\infty$$

where ω is the angular rotation speed of the disk. Following procedures adopted by Kármán,[25] the momentum and mass conservation equations defined in Eq. [1] can be satisfied by taking

$$u=\omega r F(\zeta),\ v=\omega r G(\zeta),\ w=\sqrt{\nu\omega}H(\zeta),\quad p=\rho\nu\omega P(\zeta),\ \zeta=\sqrt{\frac{\omega}{\nu}}z \qquad [2]$$

where F, G, H, and P are functions of the dimensionless variable ζ. The subsequent substitution of Eq. [2] into Eq. [1] results in a set of ordinary differential equations:

$$\left.\begin{aligned}
F^2-G^2+HF&=F''\\
2FG+HG'&=G''\\
2F+H'&=0\\
-HH'-2F'&=P'
\end{aligned}\right\}\qquad[3]$$

where the single and double primes denote the first- and second-order derivatives with respect to ζ, respectively. The initial boundary conditions can then be redefined as

$$F=0,\ G=1,\ H=0 \qquad \text{at } \zeta=0 \qquad [4]$$

$$F=0,\ G=0,\ H\neq 0,\ F'=0,\ G'=0,\ H'=0 \qquad \text{at } \zeta=\infty$$

Integrating the first two equations of Eq. [3] between 0 and ∞ and using the relations

$$\left.\begin{aligned}
\int_0^\infty HF'\,d\zeta&=[HF]_0^\infty-\int_0^\infty H'F\,d\zeta=2\int_0^\infty F^2\,d\zeta\\
\int_0^\infty HG'\,d\zeta&=[HG]_0^\infty-\int_0^\infty H'G\,d\zeta=2\int_0^\infty FG\,d\zeta
\end{aligned}\right\}$$

together with $F'(\infty)=0$ and $G'(\infty)=0$, yields

$$\left.\begin{aligned} \int_0^\infty (3F^2 - G^2)\, d\zeta &= -F'(0) \\ 4\int_0^\infty FG d\zeta &= -G'(0) \end{aligned}\right\} \quad [5]$$

For real functions F, G, H, and P, further boundary conditions obtained by differentiating Eq. [3] need to be satisfied. However, since we are principally concerned with the velocity components, second- and higher order derivatives can be ignored without encountering major errors. Based on these assumptions, reasonable approximations can be achieved by substituting trial functions for F and G such that the equations depicted in Eq. [5] and the boundary conditions listed in Eq. [4] are satisfied. The terms H and P can then be obtained by integrating the third and final components of Eq. [3].

B. *Liquid Metal Flow Prior to the Hydraulic Jump ($r < r_j$)*

Liquid metal flow prior to a hydraulic jump largely depends on the pouring conditions since the velocity of the liquid metal stream immediately prior to impingement with the atomizing disk varies with the metallostatic head, which is the distance between the disk and the top surface of the liquid metal reservoir supplying the nozzle. Assuming that the liquid metal falls freely under gravity, the velocity of the liquid metal just prior to impingement is predominantly axial and has a value $w_0 = \sqrt{2gh}$, where g is the acceleration due to gravity (9.8 m/s^2) and h is the metallostatic head. Work conducted by Cochran[26] has shown that at the high rotational speeds used in centrifugal atomization, this velocity will reduce rapidly to zero over a thin boundary layer immediately close to the disk surface. Since the thickness of this boundary layer is very small compared to the metallostatic head, the axial velocity above this layer may be considered constant and can be equated to the free fall velocity w_0. This imposes an additional boundary condition on Eq. [3] such that at $z = \infty$, $w = w_0$, or rather

$$H = -\frac{w_0}{\sqrt{\nu\omega}} \qquad \text{at } \zeta = \infty$$

The simplest functions of F, G, and H in exponential form satisfying this condition and the initial boundary conditions listed in Eq. [4] are

$$\left.\begin{aligned} F &= e^{-m\zeta}\left(a + (3mc - 4a)e^{-m\zeta} + 3(a - mc)e^{-2m\zeta}\right) \\ G &= e^{-m\zeta} \\ H &= -c + \frac{e^{-m\zeta}}{m}\left(2a + (3mc - 4a)e^{-m\zeta} + 2(a - mc)e^{-2m\zeta}\right) \end{aligned}\right\}$$

where $c = \frac{w_0}{\sqrt{\nu\omega}}$, and a and m are constants. Because F and G have to satisfy two equations in Eq. [4], a and m can be determined numerically for any given kinematic viscosity ν, initial axial velocity w_0, and disk rotation speed ω. If $c >> 1$, which is usually the case under practical atomizing conditions, $a \approx 3k(1 - k)c^2$ and $m \approx kc$, where $k \approx 0.587$. On this basis, the radial, tangential, and axial components of the liquid metal velocity as a function of the axial and radial distances from the disk can be expressed as

$$\left.\begin{aligned} u &\approx \frac{3kw_0^2 r}{\nu} e^{-\frac{kw_0}{\nu}z}\left[(1 - k) + (4k - 3)e^{-\frac{kw_0}{\nu}z} + (2 - 3k)e^{-\frac{2kw_0}{\nu}z}\right] \\ v &\approx \omega r e^{-\frac{kw_0}{\nu}z} \\ w &\approx -w_0\left(1 - e^{-\frac{kw_0}{\nu}z}\left(6(1 - k) + 3(4k - 3)e^{-\frac{kw_0}{\nu}z} + 2(2 - 3k)e^{-\frac{2kw_0}{\nu}z}\right)\right) \end{aligned}\right\} \quad [6]$$

Since, during atomization, the volume flow rate of the liquid at any radius remains a constant equal to that from the pouring nozzle, the height of liquid metal on the disk as a function of the radius can be determined by

$$Q = \int_0^{\delta_1} 2\pi r u dz = \pi r^2 w_0\left(1 - e^{-\frac{kw_0}{\nu}\delta_1}\right)^2\left(1 - 2(2 - 3k)e^{-\frac{kw_0}{\nu}\delta_1}\right) \quad [7]$$

where Q is the volume flow rate and δ_1 is the height of the liquid. Because Eq. [7] is a cubic equation of $e^{-\frac{kw_0}{\nu}\delta_1}$, δ_1 as a function of radius r can be expressed explicitly by the volume flow rate Q, initial axial velocity w_0, and kinematic viscosity ν. Because the expression is often too complicated, a more practical route is to solve Eq. [7] numerically. When $r > 5r_0$, where $r_0 = \sqrt{\frac{Q}{\pi w_0}}$ is the radius of the liquid stream just before it impinges on the disk, $e^{-\frac{kw_0}{\nu}\delta_1}$, should approach unity, *i.e.*, $\frac{kw_0\delta_1}{\nu} << 1$, to satisfy Eq. [7]. Taking the approximation $e^{-x} \approx 1 - x$ ($x << 1$), the liquid height at $r > 5r_0$ can then be calculated approximately by

$$\delta_1 \approx \frac{\nu}{kw_0 r}\sqrt{\frac{Q}{3\pi(2k - 1)w_0}} = \frac{\nu}{kw_0\sqrt{3(2k - 1)}}\frac{r_0}{r} \quad [8]$$

C. *Liquid Metal Flow after the Hydraulic Jump ($r > r_j$)*

Liquid flow after a hydraulic jump is not affected by upstream flow conditions before the jump but by the downstream flow conditions.[18] Assuming that flow is comparable to that above a rotating disk fully immersed in a liquid bath contained in an infinitely large tank, the flow behavior depends primarily on the rotation speed of the disk and on the physical properties of the liquid. Therefore, there are no further boundary conditions other than the initial ones listed in Eq. [4]. In this instance, the simplest functions of F, G, and H, again in exponential form, satisfying these conditions are

$$\left.\begin{aligned} F &= be^{-n\zeta}(1 - e^{-n\zeta}) \\ G &= e^{-n\zeta} \\ H &= -\frac{b}{n}(1 - e^{-n\zeta})^2 \end{aligned}\right\}$$

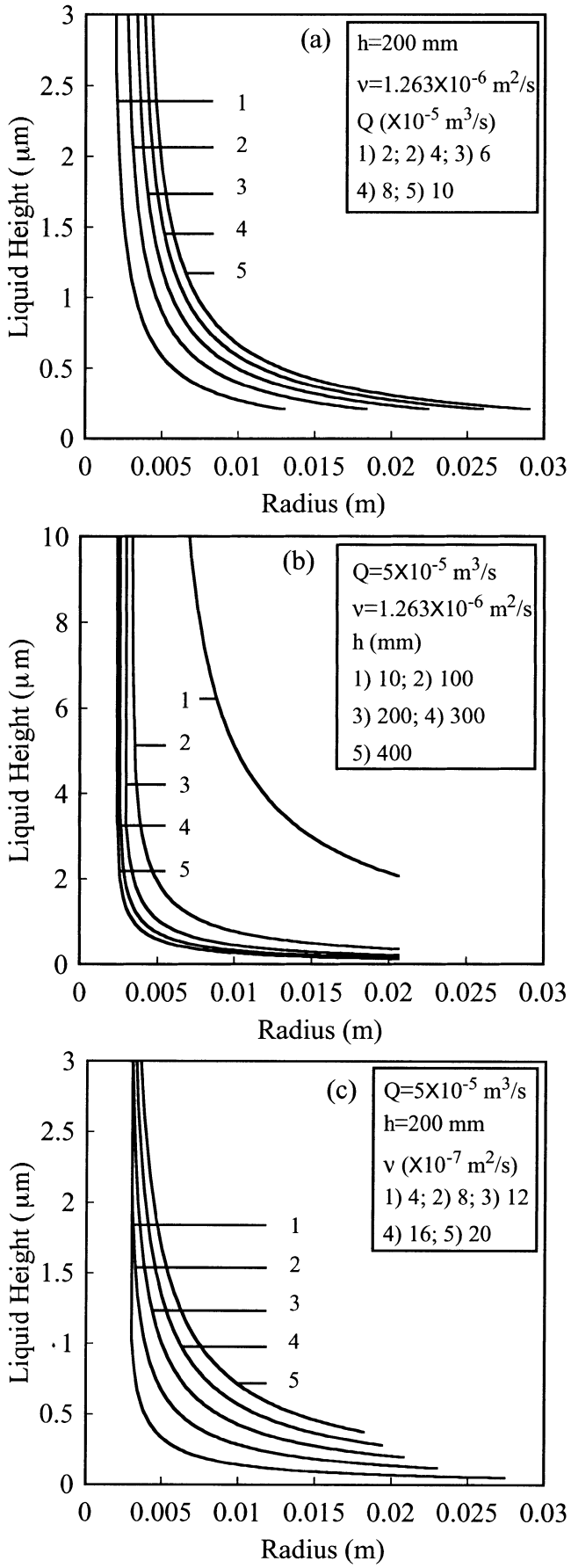

Fig. 3—Variation of liquid height with radius prior to hydraulic jump with different (*a*) volume flow rates, (*b*) metallostatic heads, and (*c*) kinematic viscosities.

where b and n are constants. With the two equations in Eq. [5] to be satisfied, b and n are calculated to be $b = 0.739$ and $n = 0.702$. The radial, tangential, and axial velocities of the liquid as a function of radial and axial distance from the disk are therefore

$$\left.\begin{aligned} u &= b\omega r e^{-n\sqrt{\frac{\omega}{\nu}}z}\left(1 - e^{-n\sqrt{\frac{\omega}{\nu}}z}\right) \\ v &= \omega r e^{-n\sqrt{\frac{\omega}{\nu}}z} \\ w &= -\frac{b}{n}\left(1 - e^{-n\sqrt{\frac{\omega}{\nu}}z}\right)^2 \end{aligned}\right\} \quad [9]$$

The volume flow rate of the liquid remains constant at any radius after the hydraulic jump and is given by integrating radial velocity u from 0 to the liquid height δ_2:

$$Q = \int_0^{\delta_2} 2\pi r u dz = \frac{b\pi r^2\sqrt{\nu\omega}}{n}\left(1 - e^{-n\sqrt{\frac{\omega}{\nu}}\delta_2}\right)^2$$

The height of the liquid δ_2 as a function of radius after the hydraulic jump can therefore be expressed by

$$\delta_2 = -\frac{1}{n}\sqrt{\frac{\nu}{\omega}}\ln\left(1 - \sqrt{\frac{nQ}{\pi b\sqrt{\nu\omega}}}\frac{1}{r}\right) \quad [10]$$

which is valid provided $r > \sqrt{\frac{nQ}{\pi b\sqrt{\nu\omega}}}$

D. *Location of the Hydraulic Jump*

If a hydraulic jump occurs on a rotating disk, the surface discontinuity of the liquid flow should form a circle at a certain critical radius r_c. Around this circle, provided energy losses are ignored,[18] the net rate of outflow of momentum of the liquid flow across the hydraulic jump is balanced by the force resulting from the pressure difference between a low liquid height before the jump and a high liquid height after the jump. At the jump radius r_c, the following equation developed from radial momentum conservation should be satisfied:[18]

$$\tfrac{1}{2}g(\delta_2^2 - \delta_1^2) = \delta_1\,\overline{u}_1^2 - \delta_2\,\overline{u}_2^2$$

where δ_1 and δ_2 are the liquid heights, and $\overline{u}_1$ and $\overline{u}_2$ are the mean radial velocities at the critical radius r_c before and after the hydraulic jump, respectively. Because the mean radial velocities to give a constant volume flow rate Q are functions of the liquid heights, namely, $\overline{u}_1 = \frac{Q}{2\pi r_c\delta_1}$ and $\overline{u}_2 = \frac{Q}{2\pi r_c\delta_2}$, the preceding equation becomes

$$2g\pi^2 r_c^2\,\delta_1\delta_2\,(\delta_1 + \delta_2) = Q^2 \quad [11]$$

Substituting Eqs. [8] and [10] into Eq. [11], the relationship between the critical radius r_c and the processing conditions is

$$r_c \ln\left(1 - \sqrt{\frac{nQ}{\pi b\sqrt{\nu\omega}}}\,\frac{1}{r_c}\right)\left(\ln\left(1 - \sqrt{\frac{nQ}{\pi b\sqrt{\nu\omega}}}\,\frac{1}{r_c}\right) - \frac{n}{kw_0\, r_c}\sqrt{\frac{\nu\omega Q}{3\pi(2k-1)w_0}}\right) = \frac{kn^2\omega w_0\, Q}{2\pi^2 g\nu^2}\sqrt{3\pi(2k-1)w_0 Q} \quad [12]$$

The critical radius r_c at which the hydraulic jump takes place can be determined numerically. It follows from Eq. [11] that if the liquid height before the hydraulic jump δ_1 decreases, the liquid height after the hydraulic jump δ_2 increases. In most cases, at the hydraulic jump, δ_1 is very small and thus δ_2 is expected to be large. For this to be the case then, the term $1 - \sqrt{\frac{nQ}{\pi b\sqrt{\nu\omega}}}\,\frac{1}{r_c}$ in Eq. [10] must tend toward zero. In other words, the critical radius r_c can be approximated by the expression

$$r_c = \sqrt{\frac{nQ}{\pi b\sqrt{\nu\omega}}} \quad [13]$$

III. DISCUSSION

A. *Liquid Height on the Disk*

As indicated by Eqs. [7] and [8], the height profile of liquid metal on the atomizing disk prior to the hydraulic jump is governed primarily by the kinematic viscosity, the volume flow rate, and the initial axial velocity of the liquid impinging on the disk, but is independent of the disk rotation speed. For the free fall bottom pouring configuration commonly used in the centrifugal atomization and spray deposition of liquid metals, the initial axial velocity of the liquid is determined by the metallostatic head, h. Figures 3(a) through (c) show the variations in liquid height with radius prior to the hydraulic jump under different volume flow rates, metallostatic heads, and kinematic viscosities, respectively, calculated by solving Eq. [7] for liquid Ti-48Al-2Mn-2Nb. At a superheat of 50 °C above the melting point, the liquid metal has a specific density $\rho = 3800$ kg/m^3 and an estimated viscosity $\mu = 0.0048$ kg/m·s and thus a kinematic viscosity $\nu = 1.263 \times 10^{-6}$ m^2/s.[29] With decreasing liquid temperature during atomization, however, the kinematic viscosity increases. For this reason and in order to determine the sensitivity of the analysis, for each parameter varied in Figures 3(a) through (c), the remaining two parameters are maintained constant: volume flow rate $Q = 5 \times 10^{-5}$ m^3/s, metallostatic head $h = 200$ mm, or kinematic viscosity $\nu = 1.263 \times 10^{-6}$ m^2/s. Assuming that the liquid stream between the nozzle and the atomizing disk is continuous, the radius of the liquid stream just before impingement increases with increasing volume flow rate and with decreasing metallostatic head. After impingement on the disk, the liquid flows radially as the axial momentum is transferred into radial momentum. For a fixed processing condition, the liquid height decreases gradually on moving radially outward from the center of the disk. Similarly for any given radial position, the height of liquid metal on the disk increases with increasing volume flow rate, with decreasing metallostatic head, and with increasing kinematic viscosity. In general, the height of liquid metal on the disk prior to the hydraulic jump is very small. With a liquid volume flow rate between 2×10^{-5} and 1×10^{-4} m^3/s, a metallostatic head between 10 to 400 mm, and a kinematic viscosity between 4×10^{-7} and 2×10^{-6} m^2/s, the liquid height beyond a radius of 0.01 m ranges from 0.05 to 5.18 μm.

The location of the hydraulic jump and the height of liquid metal on the disk after the jump depend on the kinematic viscosity of the liquid, the volume flow rate, and the disk rotation speed, but is not affected by the initial axial velocity of the liquid and therefore the metallostatic head, as can be seen from Eqs. [10] and [11]. Figures 4(a) through (c) show the variations in the liquid height with radius after the hydraulic jump under different volume flow rates, disk rotation speeds, and kinematic viscosities, respectively, with the remaining two parameters maintained constant: volume flow rate $Q = 5 \times 10^{-5}$ m^3/s, disk rotation speed $\omega = 1000$ radian/s, or kinematic viscosity $\nu = 1.263 \times 10^{-6}$ m^2/s. The radius at which the hydraulic jump takes place increases with increasing volume flow rate, with decreasing disk rotation speed, and with increasing kinematic viscosity, and varies between 0.013 and 0.028 m in the range of conditions investigated. With increasing radius from the critical hydraulic jump position, the liquid height decreases gradually. At a certain disk radius, the liquid height increases with increasing volume flow rate and decreasing disk rotation speed. The influence of kinematic viscosity on the liquid height is less significant. The liquid height after the hydraulic jump is substantially higher than that before the hydraulic jump, primarily because of the transition from rapid to a more tranquil mode of flow and because of the energy losses associated with the strong turbulence in the region of the hydraulic jump. For a volume flow rate between 2×10^{-5} and 1×10^{-4} m^3/s, a disk rotation speed between 400 and 2000 radian/s, and a kinematic viscosity between 4×10^{-7} and 2×10^{-6} m^2/s, the liquid height at a radius of 0.05 m ranges from 15.30 to 58.54 μm.

At a hydraulic jump, a large increase in liquid height is predicted in order to balance the momentum change. In practice, however, the liquid height immediately after the jump tends to be much smaller than that indicated in Figure 4 because of the strong turbulence that accompanies the jump. The variation in liquid height in the immediate vicinity of the hydraulic jump is not smooth and cannot be predicted theoretically. Fortunately, the width of this region is small and the rapid change in height that coincides with the jump has no practical significance provided that the hydraulic jump position does not coincide with the disk radius. It will, nevertheless, result in an increased height of liquid metal on the disk and therefore will have a direct effect on the droplet size distribution after atomization.

B. *Liquid Metal Velocities*

The radial and tangential components of the liquid velocity have dominant effects on the mode and rate of liquid atomization at the periphery of the disk and will ultimately determine the amount of premature solidification and skull buildup on the disk. As indicated by Eqs. [6] and [9], both the radial and tangential velocities are complex functions of the radial and axial distances from the disk. At the in-

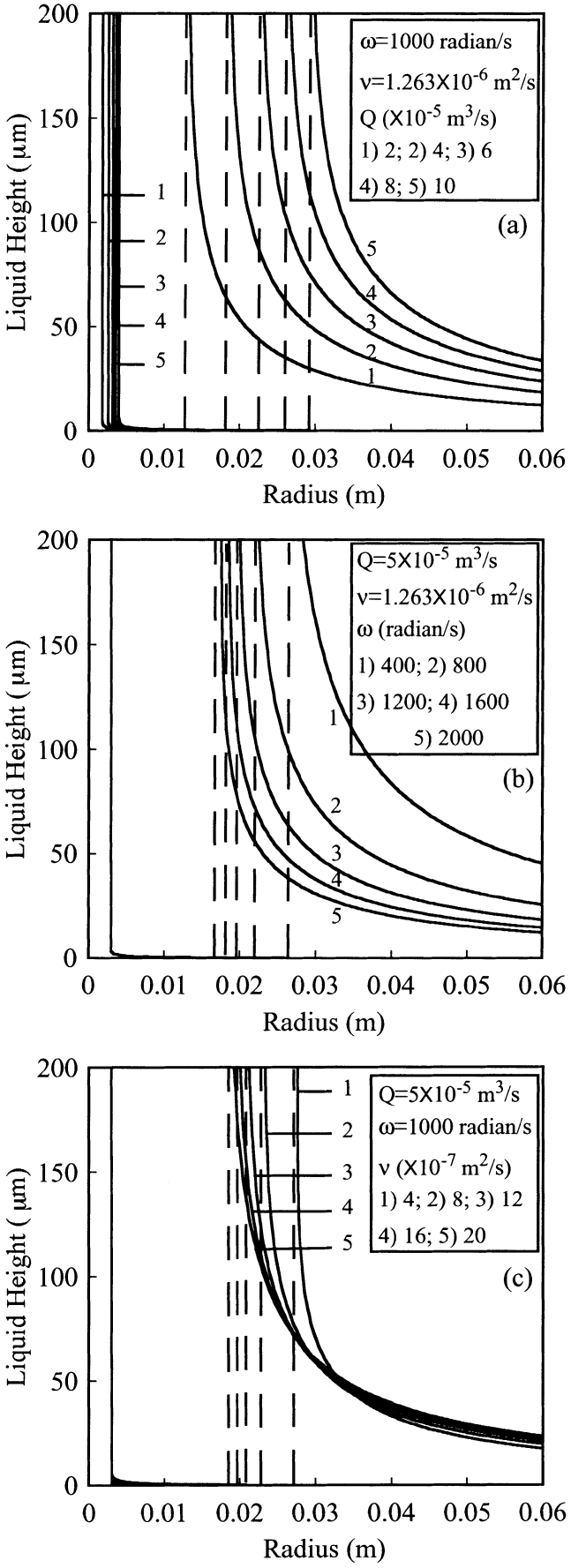

Fig. 4—Variation of liquid height with radius after hydraulic jump with different (*a*) volume flow rates, (*b*) disk rotation speeds, and (*c*) kinematic viscosities.

terface between the liquid metal and the disk, the liquid has a zero velocity relative to the atomizing disk. However, as the axial distance is increased, both the radial and tangential velocities relative to the disk increase. The important parameters in terms of centrifugal atomization would appear to be the mean radial and tangential velocities as a function of disk radius. The mean radial velocity at a radius r to give an equivalent constant volume flow rate Q is $\overline{u} = \frac{Q}{2\pi r\delta}$, where δ is the liquid height. Figures 5(a) through (c) show the variations in mean radial velocity with radius prior to the hydraulic jump, under different volume flow rates, metallostatic heads, and kinematic viscosities respectively, with the remaining two parameters maintained constant: volume flow rate $Q = 5 \times 10^{-5}$ m^3/s, metallostatic head $h = 200$ mm, or kinematic viscosity $\nu = 1.263 \times 10^{-6}$ m^2/s. When the liquid impinges on the disk, axial momentum is transformed into radial momentum, accelerating the liquid rapidly up to a mean radial velocity of 5900 m/s. This extremely rapid flow accounts for the very thin liquid layer before the hydraulic jump, as shown in Figure 3. With increasing radius beyond 0.01 m, the mean radial velocity increases only slightly for a fixed processing condition. At a radius $r = 0.01$ m, the mean radial velocity increases from 1162 to 2384 m/s, from 154 to 2980 m/s, and from 1121 to 5603 m/s with increasing volume flow rate from 2×10^{-5} to 1×10^{-4} m^3/s, with increasing metallostatic head from 10 to 400 mm, and with decreasing kinematic viscosity from 2×10^{-6} to 4×10^{-7} m^2/s, respectively.

Figures 6(a) through (c) show the variations in mean radial velocity with radius after the hydraulic jump under different volume flow rates, disk rotation speeds, and kinematic viscosities, respectively, with the remaining two parameters maintained constant: volume flow rate $Q = 5 \times 10^{-5}$ m^3/s, disk rotation speed $\omega = 1000$ radian/s, or kinematic viscosity $\nu = 1.263 \times 10^{-6}$ m^2/s. Immediately after the hydraulic jump, the rapid liquid flow becomes almost quiescent due to the sudden great increase in liquid height. With increasing radius after the jump, the mean radial velocity of the liquid increases, first rapidly then steadily up to 12 m/s at a radius $r = 0.1$ m. In general, however, the mean radial velocity after the hydraulic jump is much lower than that before the jump. At a radius of 0.05 m, the mean radial velocity of the liquid increases from 4.16 to 7.18 m/s, from 2.72 to 10.44 m/s, and from 5.45 to 7.00 m/s with increasing volume flow rate from 2×10^{-5} to 1×10^{-4} m^3/s, with increasing disk rotation speed from 400 to 2000 radian/s, and with decreasing kinematic viscosity from 2×10^{-6} to 4×10^{-7} m^2/s, respectively.

The mean tangential velocity of the liquid at a certain radius can be expressed as $\overline{v} = \frac{\int_0^\delta v dz}{\delta}$. Because the mean tangential velocity is smaller than, but usually close to, that of the disk, it is often convenient to describe the deviation of the tangential velocity of the liquid from that of the disk by a parameter designated as the degree of slippage $\phi = 1 - \frac{\overline{v}}{\omega r}$, which is the ratio between the mean tangential velocity of the liquid relative to the disk and the absolute velocity of the disk. Figures 7(a) through (d) show the variations in the degree of slippage with radius for different

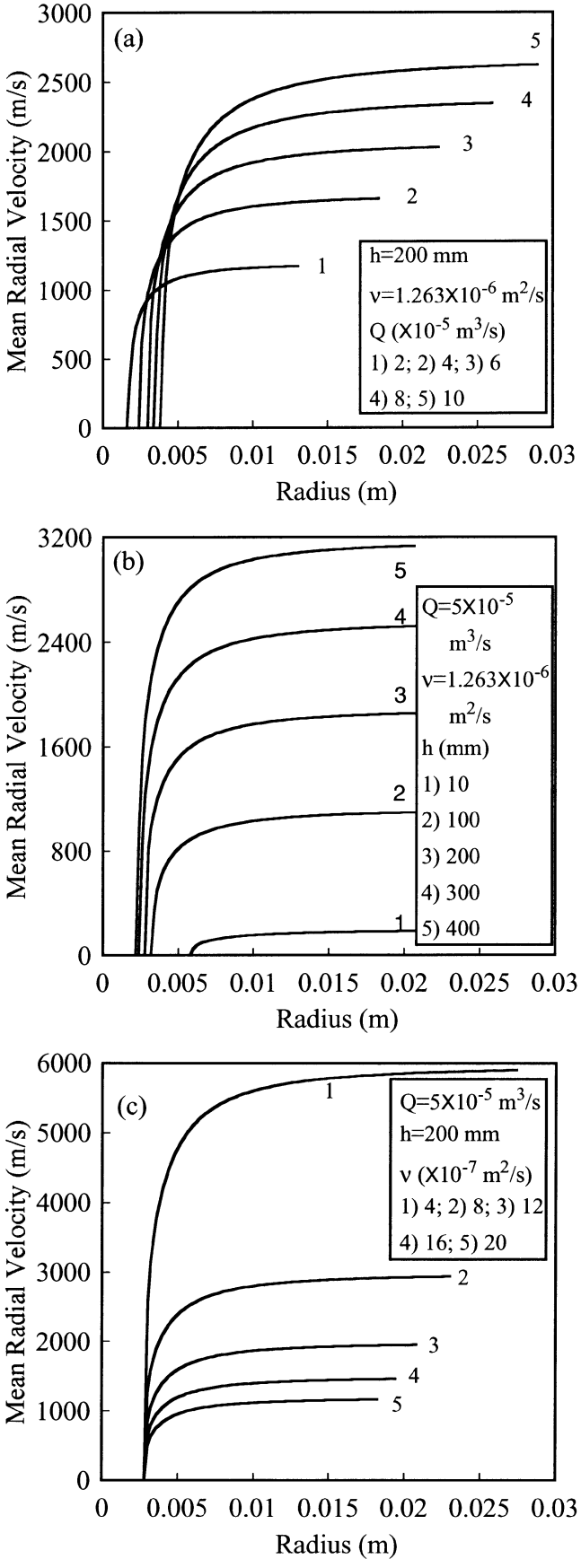

Fig. 5—Variation of mean radial velocity with radius prior to hydraulic jump with different (*a*) volume flow rates, (*b*) metallostatic heads, and (*c*) kinematic viscosities.

volume flow rates, metallostatic heads, disk rotation speeds, and kinematic viscosities, respectively, with the remaining three parameters maintained constant: volume flow rate $Q = 5 \times 10^{-5}$ m^3/s, metallostatic head $h = 200$ mm, disk rotation speed $\omega = 1000$ radian/s, or kinematic viscosity $\nu = 1.263 \times 10^{-6}$ m^2/s. The degree of slippage prior to impingement on the disk is unity since the liquid metal stream does not rotate with the disk. With the liquid flowing radially outward, the degree of slippage decreases rapidly. Immediately prior to the hydraulic jump, the degree of slippage remains constant at $\phi \approx 0.09$ regardless of variations in the volume flow rate, disk rotation speed, or kinematic viscosity, as shown in Figures 7(a), (c), and (d), but decreases from 0.56 to 0.06 with increasing metallostatic head from 10 to 400 mm, as shown in Figure 7(b). Just after the hydraulic jump, the degree of slippage is very high, and as a consequence, the mean tangential velocity is low. However, with increasing radius, the degree of slippage decreases, first rapidly and then relatively slowly. At any specified radius, the degree of slippage increases with increasing volume flow rate and with decreasing metallostatic head prior to the hydraulic jump, and increases with increasing volume flow rate, with decreasing disk rotation speed, and with decreasing kinematic viscosity after the jump. At a radius $r = 0.05$ m, the degree of slippage ranges from 0.09 to 0.33 for the range of processing conditions commonly encountered in the centrifugal atomization of liquid metals.

C. *Comparison with Experimental Observations*

Figure 8 shows the skull formed on the atomizing disk during centrifugal spray deposition of liquid Ti-48Al-2Mn-2Nb. The equipment used in this work and the experimental conditions have been reported in detail in a previous article.[29] In summary, the volume (or mass) flow rate, metallostatic head, and disk rotation speed were all maintained constant at $Q = 6.096 \times 10^{-5}$ m^3/s (13.9 kg/min), $h = 0.4$ m, and $\omega = 314.16$ radian/s (3000 rpm). It is apparent from Figure 8 that at radii less than approximately 0.03 m, there was very little solidification and/or skull buildup, despite the intense water cooling imposed at the center of the disk. The small variation in skull thickness close to the center of the disk can be attributed to two effects: the premature breakup of the liquid metal stream prior to impact with the disk and the impact of individual droplets with the disk (an effect that became pronounced toward the end of the pouring process); and the shrinkage and buckling of the solid skull at the conclusion of the pouring operation. Beyond 0.03 m, however, extensive solidification had occurred, resulting in a large doughnut-shaped skull. The sharp increase in skull thickness at $r = 0.03$ m has been assumed to be coincident with the occurrence of a hydraulic jump in the flow of liquid metal on the disk, as indicated in Figure 1. This assumption has been rationalized on the basis that in the absence of a hydraulic jump, the cooling condition on the disk would be expected to promote a relatively smooth transition in skull thickness on moving from the center to the edge. In fact the combination of water jet cooling with high rotation speeds means that temperature differentials in the radial direction are small. This, combined with the gradual decrease in liquid metal temperature, would not be expected to result in the pronounced thickness variations

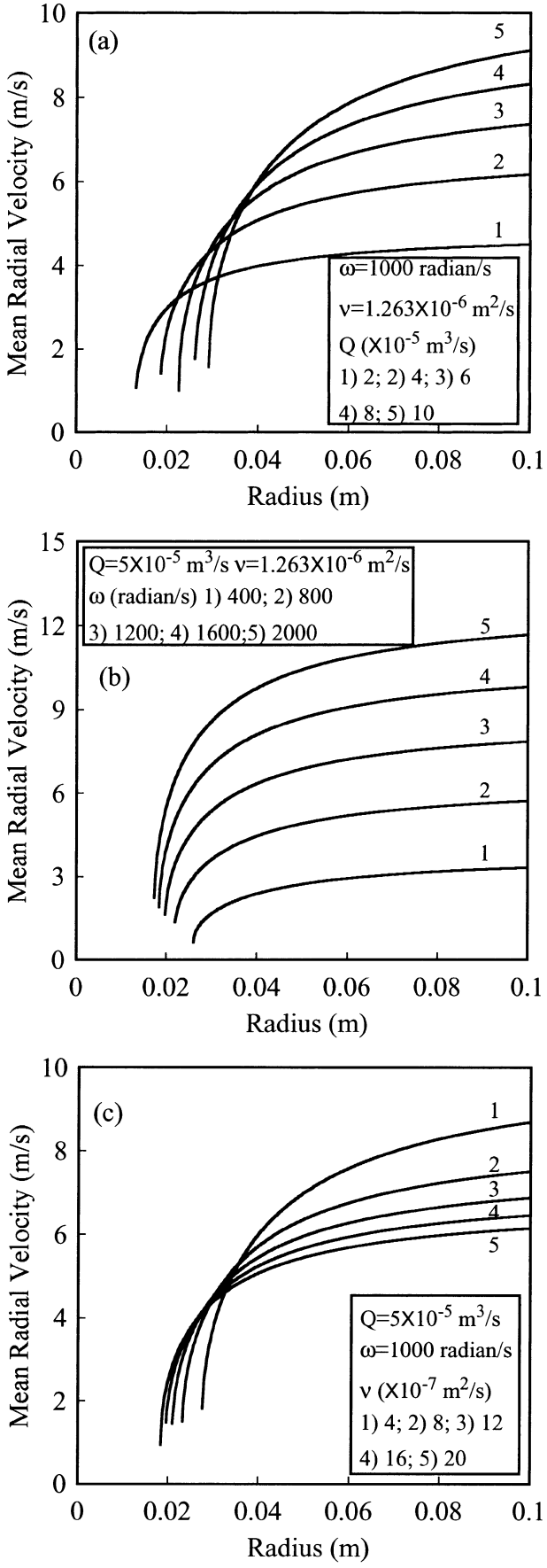

Fig. 6—Variation of mean radial velocity with radius after hydraulic jump with different (*a*) volume flow rates, (*b*) disk rotation speeds, and (*c*) kinematic viscosities.

illustrated in Figure 8. Substituting the process conditions into the model, a hydraulic jump would be expected to take place at $r = 0.0304$ m. This agrees well with the sharp increase in skull thickness at $r = 0.03$ m, as shown in Figure 8. Before the hydraulic jump takes place, liquid metal flow on the disk is rapid, with a mean radial velocity as high as 3432 m/s, as calculated from Eq. [7], and a height as low as 0.1 μm. In this respect, the short residence time of the liquid on the disk restricts solidification to a thin boundary layer immediately adjacent to the disk surface. In direct contrast, the mean radial velocity after the jump decreases significantly, typically to less than 1.5 to 2.3 m/s, and the liquid height increases to in excess of 85 to 184 μm. As a result, the heat transfer to the disk is enhanced, resulting in an increase in the rate of solidification and a net buildup in skull thickness.

Recent studies conducted by Zhao *et al.*[29] have shown that the flow lines observed on the skull after atomization can be related directly to the flow of liquid metal on the atomizing disk. Specifically, the angular variation in the liquid trajectory with radius depends on the ratio between the mean tangential and radial velocities relative to the disk and follows the relation

$$\frac{r\,d\theta}{dr} = \frac{\omega r - \bar{v}}{\bar{u}}$$

On this basis, the flow lines on the skull can be used to evaluate the accuracy of the velocity calculations. It should be noted, however, that flow lines were not visible at radii less than 0.03 m, and as a consequence, it was not possible to validate the flow calculations prior to the hydraulic jump. Following a flow line after the hydraulic jump on the skull in Figure 8, the angular coordinates at a series of radii are measured. Figure 9 compares the experimental measurements of the liquid metal trajectory with predicted values calculated using both the present jump model and a ''shear stress'' analytical model originally proposed by Zhao *et al.*[29] The trajectory predicted by the jump model using velocity values obtained from Eq. [9] agrees well with the experimental data provided the radius is smaller than 0.045 m. Beyond this value, there is considerable deviation. In contrast, the liquid metal trajectory predicted by the shear stress model shows good agreement with the experimental data at radii greater than 0.04 m but shows large deviations when the radius is smaller than this value. In reality, liquid metal trajectories calculated using the shear stress model for radii less than ≈0.03 m are meaningless, because the model does not consider the effect of the metallostatic head during pouring and therefore does not take into account the principal parameters governing flow prior to the hydraulic jump. Similarly, the degree of slippage immediately after the jump is high, as shown in Figure 7, typically exceeding 0.4. In this respect, the shear model gives poor results since it is only valid when the degree of slippage is ≤0.2.[29] In contrast, the jump model takes into account the amount of tangential slippage and therefore gives an improved correlation with the experimental data. As the radius is increased, however, the degree of slippage is reduced and, at radii greater than 0.04 m, falls to less than 0.17 at which point the shear stress model yields a better prediction. The large deviations observed with the jump model within this region probably stem from the fact that the axial, radial,

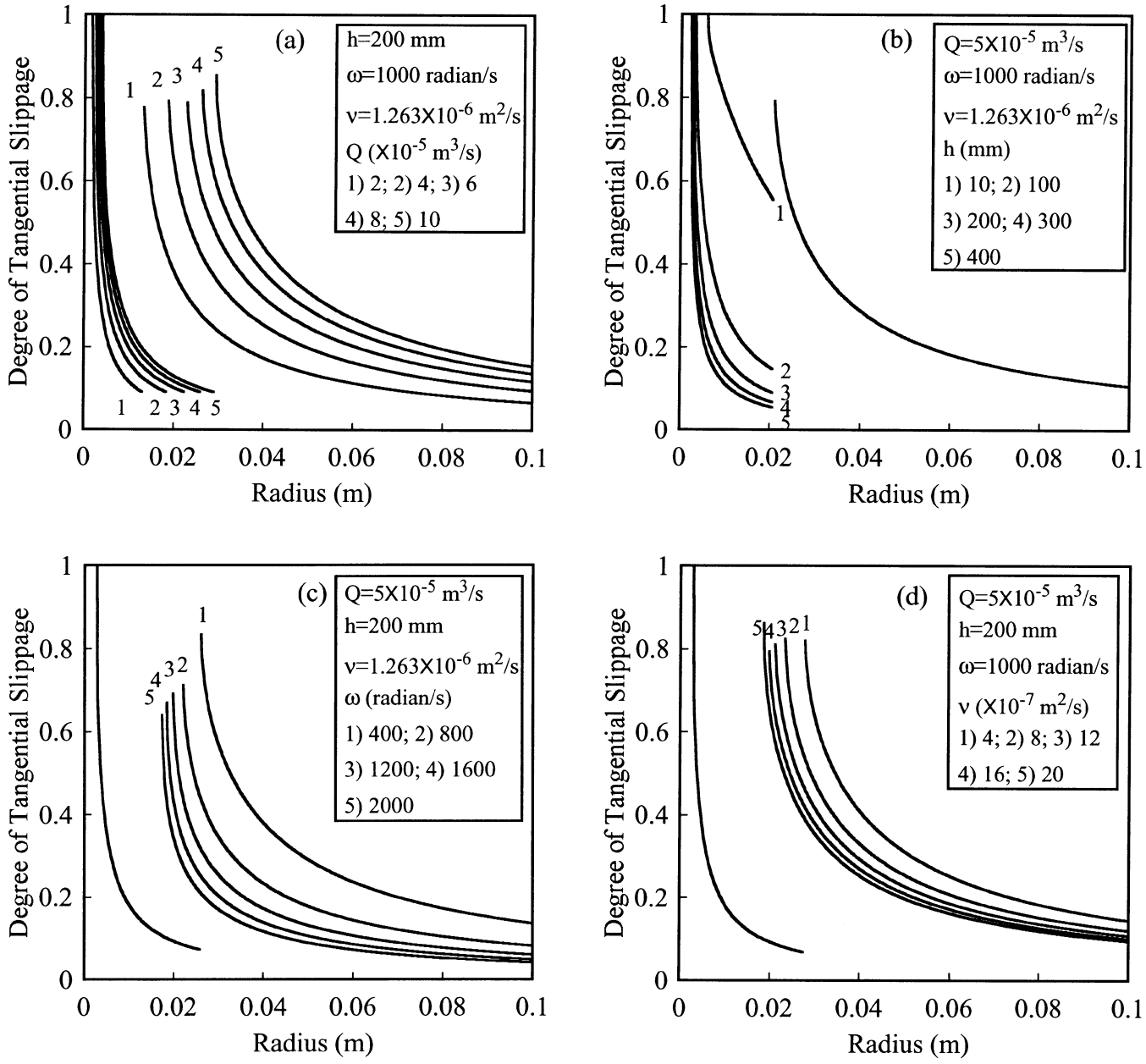

Fig. 7—Variation of degree of tangential slippage with radius with different (*a*) volume flow rates, (b) metallostatic heads, (c) disk rotation speeds, and (d) kinematic viscosities.

and tangential velocities of the liquid are approximated using trial functions, which, at the small liquid heights observed at large radii, invariably introduce some degree of error. In general, the jump model will give a reasonable approximation of the position of the hydraulic jump, and can be used to calculate the velocity distributions and the liquid metal profile on the disk, either prior to or immediately after the hydraulic jump or under conditions where there is a high degree of slippage. The shear model will invariably give more accurate results at large disk radii where the degree of slippage on the disk is low.

D. *Implications*

The metallostatic head during pouring essentially determines the initial axial velocity of the liquid impinging on the atomizing disk, which in turn affects the liquid behavior on the disk prior to the hydraulic jump. In contrast, the hydraulic jump position and the flow of liquid metal on the disk after the jump are not affected by the metallostatic head, but are rather controlled by the volume flow rate and the disk rotation speed. This implies that the pouring distance, or the distance between the nozzle and the disk, has little influence on the atomization response of the liquid at the periphery of the disk, provided the disk radius exceeds the critical radius for the occurrence of a hydraulic jump. The radius of the disk currently used in the centrifugal atomization and deposition of liquid metals is usually in the region of 0.05 m, which, for the range of pouring conditions considered to date, is beyond the critical radius for a hydraulic jump. In this respect, the apparent insensitivity of liquid metal flow to pouring distance after the hydraulic

Fig. 8—Solid skull formed on an atomizing disk.

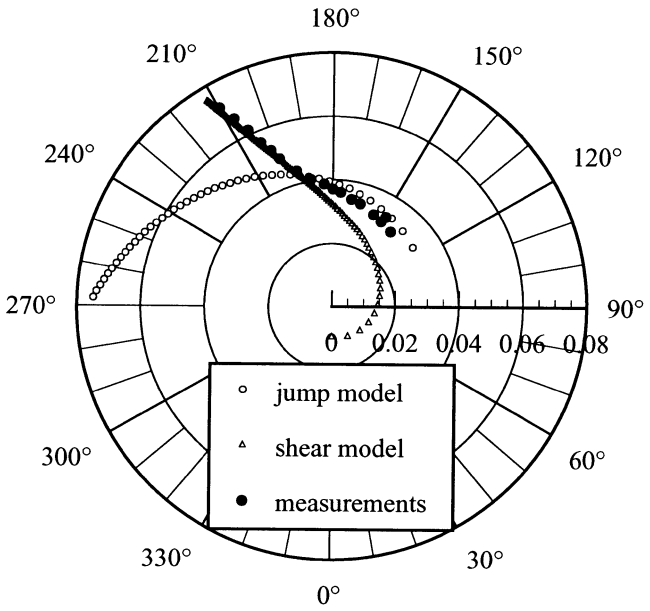

Fig. 9—Measured and calculated flow lines of the liquid metal on the atomizing disk.

jump clearly offers some benefits in terms of the atomizer and pouring system design. During centrifugal spray deposition, the atomized droplets are normally directed on to the surface of a cylindrical substrate, which is configured in such a way as to reciprocate vertically in the path of the spray, thus allowing the controlled buildup of deposit shape. With this configuration, the melting crucible and pouring system need to be kept well above the disk, in order to avoid interference with the substrate manipulation facilities and to allow the production of rings with extended axial lengths. However, as the pouring distance increases, there is a tendency for the melt stream to break up prior to impact the disk, resulting in periodic variations in the liquid volume flow rate. In the absence of a hydraulic jump, this would invariably give rise to variability in the droplet size distribution with knock-on effects in terms of the microstructure and surface quality of the deposit. Such effects are not retained after the hydraulic jump because of the strong mixing that occurs within the transition region and because of the change from turbulent to a more quiescent mode of flow. These benefits do, however, need to be balanced against the increased liquid metal thickness on the disk and the attendant reductions in radial velocity, since both of these effects will tend to result in an increase in the average droplet size. Under the processing conditions investigated to date, the liquid height and the mean radial and maximum tangential velocities prior to ($r = 0.01$ m) and after the jump ($r = 0.05$ m) would be expected to vary in the ranges 0.1 to 6 μm and 15 to 60 μm, 150 to 3100 m/s and 2 to 10 m/s, and 4 to 20 m/s and 20 to 100 m/s. The liquid flow is therefore mainly radial before the hydraulic jump and tangential after the jump. If a small atomizing disk is used in order to prevent the hydraulic jump, the combination of small liquid height and high radial velocity would be expected to lead to the formation of smaller droplets at the disk edge. This is clearly beneficial in that smaller liquid droplets have higher cooling rates during flight and can result in more uniform deposit microstructures. However, since the liquid height and the mean radial velocity prior to a hydraulic jump are controlled primarily by the liquid volume flow rate and by the metallostatic head, some variability might be expected, particularly at extended pouring distances, due to the premature breakup of the melt stream and the increased splatter associated with the impact of individual droplets on the disk. Further work is clearly required in order to resolve these issues.

IV. CONCLUSIONS

During centrifugal atomization and spray deposition of liquid metals, a hydraulic jump from a rapid flow to a tranquil flow often takes place on the atomizing disk. A mathematical model has been developed in order to predict the occurrence and location of this jump and the associated variations of liquid metal height profile on the disk and the changes in radial and tangential velocities as functions of the liquid kinematic viscosity ν, the volume flow rate Q, the metallostatic head h, and the disk rotation speed ω. Under the conditions commonly encountered during processing, $\nu = 1.263 \times 10^{-6}$ m^2/s, $Q = 2 \times 10^{-5}$ to 1×10^{-4} m^3/s, $h = 10$ to 400 mm, and $\omega = 1000$ radian/s, the liquid height and the mean radial velocity vary in the range of 0.1 to 6 μm and 150 to 3000 m/s before the hydraulic jump and 15 to 60 μm and 2 to 10 m/s after the jump. The degree of tangential slippage between the liquid and the disk varies in the range of 0.1 to 0.5, except at the point of impingement and in regions close to the hydraulic jump. Increasing the liquid volume flow rate increases the height of liquid metal on the disk, the critical hydraulic jump radius, the mean radial velocity, and the degree of slippage. Increasing the metallostatic head or the pouring distance reduces the height of liquid metal on the disk and the degree of slippage and increases the mean radial velocity prior

to the hydraulic jump, but does not affect the hydraulic jump position or the liquid behavior after the jump. Increasing the disk rotation speed reduces the liquid height and the critical radius and increases the mean radial velocity and the degree of slippage after the hydraulic jump, but does not affect these parameters before the hydraulic jump. Increasing the liquid kinematic viscosity increases the liquid height and decreases the critical radius, the mean radial velocity, and the degree of slippage after the hydraulic jump, but does not affect the degree of slippage before the hydraulic jump. The model can explain the formation of the doughnut-shaped skull that forms on the disk during atomization. The calculations of hydraulic jump position and liquid trajectories after a hydraulic jump agree well with measurements of the flow lines on the skull when the radius is smaller than 0.045 m. The model implies that a small atomizing disk preventing hydraulic jump favors formation of fine spray droplets.

ACKNOWLEDGMENTS

The authors acknowledge the support of their colleagues in the Plasma Melting and Spray Forming group at the IRC. In particular, thanks are due to Mr. R.M. Ward, Dr. T.P. Johnson, and Dr. X.G. Yang for their encouragement and helpful discussions. Funding for this work was provided by the United Kingdom Engineering and Physical Sciences Research Council.

TABLE OF SYMBOLS

a	constant
b	constant
c	variable related to w_o, ν, and ω
F	trial function for radial velocity
G	trial function for tangential velocity
g	gravitational acceleration
H	trial function for axial velocity
h	metallostatic head
k	constant
m	constant
n	constant
P	trial function for pressure
p	pressure
Q	liquid volume flow rate
r	radial distance
r_0	radius of liquid stream at impingement
r_c	critical radius of hydraulic jump
u	radial velocity
$\overline{u}$	mean radial velocity
$\overline{u}_1$	mean radial velocity at r_c before hydraulic jump
$\overline{u}_2$	mean radial velocity at r_c after hydraulic jump
v	tangential velocity
$\overline{v}$	mean tangential velocity
w	axial velocity
w_o	initial axial velocity
z	axial distance
δ	liquid height
δ_1	liquid height before hydraulic jump
δ_2	liquid height after hydraulic jump
ϕ	degree of tangential slippage
μ	viscosity
ν	kinematic viscosity
θ	polar angle
ρ	specific density
ω	disk rotation speed
ζ	dimensionless variable related to z, ν, and ω
∇^2	mathematical operator

REFERENCES

1. P.S. Grant: *Progr. Mater. Sci.*, 1995, vol. 39, pp. 497-545.
2. A. Leatham: *Mater. World*, 1996, vol. 4, pp. 317-20.
3. E.S. Huron: *Spray Forming 2—Proc. 2nd Int. Conf. on Spray Forming*, J.V. Wood, ed., Woodhead Publishing, Cambridge, United Kingdom, 1993, pp. 155-64.
4. P.D. Prichard and R.P. Dalal: in *Superalloys 1992*, S.D. Antolovich, R.W. Stusrud, R.A. Mackay, D.L. Anton, T. Khan, R.D. Kissinger, and D.L. Klarstrom, eds., TMS, Warrendale, PA, 1992, pp. 205-14.
5. D. Briant, R.P. Dalal, and D. Furrer: *Total Technology for Advanced Materials—Proc. 3rd Int. Conf. on Spray Forming*, Osprey Metals Ltd., Cardiff, United Kingdom, 1997, pp. 79-88.
6. H.C. Fiedler, T.F. Sawyer, R.W. Kopp, and A.G. Leatham: *J. Met.*, 1987, vol. 39, pp. 28-33.
7. M.H. Jacobs, J.M. Young, A.L. Dowson, and M.A. Ashworth: in *Advances in Powder Metallurgy and Particulate Materials—1995*, M. Phillips and J. Porter, eds., Metal Powder Industries Federation, Princeton, NJ, 1995, vol. 2, pp. 7.57-7.71.
8. A.R.E. Singer and S.E. Kisakurek: *Met. Technol.*, 1976, pp. 565-70.
9. B.A. Rickinson, F.A. Kirk, and D.R.A. Davies: *Powder Metall.*, 1981, vol. 24, pp. 1-6.
10. M.G. Osborne, I.E. Anderson, K.S. Funke, and J.D. Verhoeven: in *Powder Production and Spray Forming: Advances in Powder Metallurgy and Particulate Materials—1992*, J.M. Capus and R.M. German, eds., Metal Powder Industries Federation, Princeton, NJ, 1992, pp. 89-103.
11. R. Angers: in *Powder Production and Spray Forming: Advances in Powder Metallurgy and Particulate Materials—1992*, J.M. Capus and R.M. German, eds., Metal Powder Industries Federation, Princeton, NJ, 1992, pp. 79-88.
12. D.R.G. Davies and A.R.E. Singer: in *Powder Production and Spray Forming: Advances in Powder Metallurgy & Particulate Materials—1992*, J.M. Capus and R.M. German, eds., Metal Powder Industries Federation, Princeton, NJ, 1992, pp. 301-17.
13. J.W. Sears, G. Itoh, and M.H. Loretto: in *Titanium '92: Science and Technology*, F.H. Froes and I. Caplan, eds., TMS, Warrendale, PA, 1993, vol. 2, pp. 987-1002.
14. A.L. Dowson, M.A. Duggan, Y.Y. Zhao, M.H. Jacobs, and J.M. Young: in *Advances in Powder Metallurgy & Particulate Materials—1996*, T.M. Cadle and K.S. Narasimhan, eds., Metal Powder Industries Federation, Princeton, NJ, 1996, vol. 3, pp. 9/67-9/98.
15. A.L. Dowson, M.H. Jacobs, J.M. Young, Y.Y. Zhao, B. Parsons, D. Weale, and M. Bird: in *Total Technology for Advanced Materials—Proc. 3rd Int. Conf. on Spray Forming*, Osprey Metals Ltd., Cardiff, United Kingdom, 1997, pp. 193-202.
16. R.P. Fraser, E.P. Eisenklam, and N. Dombrowski: *Br. Chem. Eng.*, 1957, pp. 496-501.
17. K. Masters: *Spray Drying Handbook*, 5th ed., Longman Scientific & Technical, Longman Group UK Ltd., Essex, England, 1991, p. 203.
18. J.M. Kay and R.M. Nedderman: *An Introduction To Fluid Mechanics And Heat Transfer*, 3rd ed., Cambridge University Press, Cambridge, United Kingdom, 1974, p. 246.
19. R.W. Fox and A.T. McDonald: *Introduction to Fluid Mechanics*, 4th ed., John Wiley & Sons Inc., New York, NY, 1994, p. 722.
20. E.J. Watson: *J. Fluid Mech.*, 1964, vol. 20, pp. 481-99.
21. M.M. Rahman, W.L. Hankey, and A. Faghri: *Int. J. Heat Mass Transfer*, 1991, vol. 34, pp. 103-14.
22. R.I. Bowles and F.T. Smith: *J. Fluid Mech.*, 1992, vol. 242, pp. 145-68.
23. F.J. Higuera: *J. Fluid Mech.*, 1994, vol. 274, pp. 69-92.
24. S. Middleman: *Modeling Axisymmetric Flows—Dynamics of Films, Jets, and Drops*, Academic Press Inc., San Diego, CA, 1995, p. 125.
25. T.V. Kármán: *Z. Ang. Math. Mech.*, 1921, vol. 1, pp. 233-52.

26. W.G. Cochran: *Proc. Cambridge Phil. Soc.*, 1934, vol. 30, pp. 365-75.
27. J.T. Stuart: *Q. J. Mech. Appl. Math.*, 1954, vol. 7, pp. 446-57.
28. P.D. Ariel: *J. Appl. Mech., Trans. ASME*, 1996, vol. 63, pp. 436-38.
29. Y.Y. Zhao, A.L. Dowson, T.P. Johnson, J.M. Young, and M.H. Jacobs: in *Advances in Powder Metallurgy & Particulate Materials—1996*, T.M. Cadle and K.S. Narasimhan, eds., Metal Powder Industries Federation, Princeton, NJ, 1996, vol. 3, pp. 9/79-9/89.